# Spin Nematics, Valence-Bond Solids, and Spin Liquids in SO(N) Quantum Spin Models on the Triangular Lattice

Ribhu K. Kaul

Phys. Rev. Lett. **115**, 157202 — Published 7 October 2015

DOI: 10.1103/PhysRevLett.115.157202

# Spin nematics, valence-bond solids and spin liquids in SO($N$) quantum spin models on the triangular lattice

Ribhu K. Kaul
*Department of Physics & Astronomy, University of Kentucky, Lexington, KY-40506-0055*

We introduce a simple model of SO($N$) spins with two-site interactions which is amenable to quantum Monte-Carlo studies without a sign problem on *non-bipartite* lattices. We present numerical results for this model on the two-dimensional triangular lattice where we find evidence for a spin nematic at small $N$, a valence-bond solid (VBS) at large $N$ and a quantum spin liquid at intermediate $N$. By the introduction of a sign-free four-site interaction we uncover a rich phase diagram with evidence for both first-order and exotic continuous phase transitions.

The destruction of magnetic order by quantum fluctuations in spin systems is frequently invoked as a route to exotic condensed matter physics such as spin liquid phases and novel quantum critical points [1–3]. The most commonly studied spin Hamiltonians have symmetries of the groups SO(3) and SU(2) which describe the rotational symmetry of 3-dimensional space. Motivated both by theoretical and experimental [4] interest, spin models with larger-$N$ symmetries have been introduced, e.g. extensions of SU(2) to SU($N$) [5–8] or Sp($N$) [9].

The extension of SO(3) to SO($N$) is an independant large-$N$ enlargement of symmetry, with its own physical motivations [10]. While there have been many studies of SO($N$) spin models in one dimension [11–13], our understanding of their ground states and quantum phase transitions in higher dimension is in its infancy. To this end, we introduce here a simple SO($N$) spin model that surprisingly is sign free on *any* non-bipartite lattice. This model provides us with a new setting in which the destruction of magnetic order can be studied in higher dimensions using *unbiased* methods. As an example of interest, we present the results of a detailed study of the phase diagram of the our SO($N$) anti-ferromagnet on the two-dimensional triangular lattice.

*Models.* – Consider a triangular lattice, each site of which has a Hilbert state of $N$ states, we will denote the state of site $j$ as $|\alpha\rangle_j$ ($1 \leq \alpha \leq N$). Define the $N(N-1)/2$ generators of SO($N$) on site $i$ as $\hat{L}_i^{\alpha\beta}$ with $\alpha < \beta$; they will be chosen in the fundamental representation on all sites: $\hat{L}_j^{\alpha\beta}|\gamma\rangle_j = i\delta_{\beta\gamma}|\alpha\rangle_j - i\delta_{\alpha\gamma}|\beta\rangle_j$. Now consider the following SO($N$) [14] symmetric lattice model for $N \geq 3$,

$$\hat{H}_J = -\frac{J}{N^2 - 2N}\sum_{\langle ij\rangle}(\hat{L}_i \cdot \hat{L}_j)^2, \tag{1}$$

where the "$\cdot$" implies a summation over the $N(N-1)/2$ generators and $\langle ij\rangle$ is the set of nearest neighbors. To see that $\hat{H}_J$ does not suffer from the sign problem, define a "singlet" state on a bond, $|S_{ij}\rangle \equiv \frac{1}{\sqrt{N}}\sum_\alpha |\alpha\alpha\rangle_{ij}$ and the singlet projector $\hat{P}_{ij} = |S_{ij}\rangle\langle S_{ij}|$. Using these operators and ignoring a constant shift we find the simple form [15],

$$\hat{H}_J = -J\sum_{\langle ij\rangle}\hat{P}_{ij}. \tag{2}$$

We make four observations: First, it is possible to create an SO($N$) spin singlet with only two spins for all $N$ (in contrast to SU($N$) where $N$ fundamental spins are required to create a singlet); Second Eq. (1) being a sum of projectors on this two-site singlet is the simplest SO($N$) coupling, despite it being a biquadratic interaction in the generators $\hat{L}^{\alpha\beta}$; Third, since the singlet has a positive expansion, $\hat{H}_J$ is Marshall positive on *any* lattice; Fourth, on bipartite lattices $\hat{H}_J$ is equivalent to the familiar SU($N$) anti-ferromagnet [6], i.e. the obvious SO($N$) of Eq. (1) is enlarged to an SU($N$) symmetry. Since the bipartite SU($N$) case has been studied in great detail in past work on various lattices [7, 16–23], we shall concern ourselves here with the non-bipartite SO($N$) case which is relatively unexplored.

*Phases of $\hat{H}_J$:* Starting at $N = 3$, Eq. (1) becomes $\hat{H} = -\frac{J}{3}\sum_{\langle ij\rangle}\left(\vec{S}_i \cdot \vec{S}_j\right)^2$ with $\vec{S}$ the familiar $S = 1$ representation of angular momentum. Previous numerical work has shown that this triangular lattice $S = 1$ biquadratic model [24, 25] has an SO(3) symmetry breaking "spin nematic" magnetic ground state (we shall denote this phase by SN). The ground state of $\hat{H}_J$ for $N > 3$ has not been studied in the past.

In the large-$N$ limit, analogous to previous work for SU($N$) anti-ferromagnets on bipartite lattices [26], the ground state is infinitely degenerate and consists of dimer coverings where each dimer is in $|S_{ij}\rangle$. At leading order in $1/N$, $\hat{H}_J$ introduces off-diagonal moves which re-arrange parallel dimers around a plaquette, mapping $\hat{H}_J$ at large-$N$ to a quantum dimer model on the triangular lattice with only a kinetic term,

$$\hat{H}_{\rm QDM} = -t\sum_{\rm plaq}\left\{\left(|\ \rangle_i\langle\ |_i + h.c.\right)\right. \tag{3}$$

where the sum on plaquettes includes all closed loops of length four on the triangular lattice. The ground state of this model has been found in previous analytic [27] and numerical work [28] to be a $\sqrt{12}\times\sqrt{12}$ valence bond solid (VBS), breaking the lattice translation symmetry. We thus expect that at large but finite values of $N$, $\hat{H}_J$ should restore its SO($N$) symmetry and enter this same VBS state.

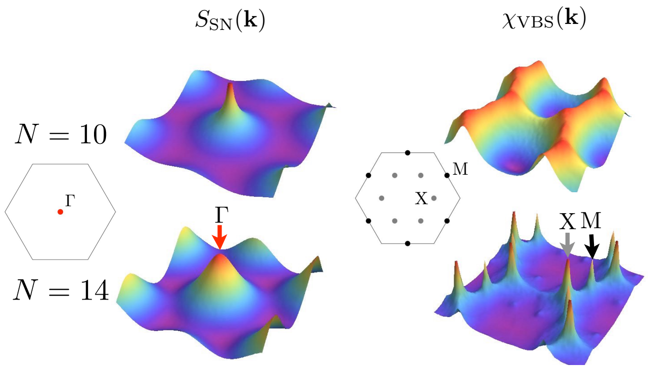


FIG. 1. Equal time structure factors for SN order $[S_{\mathrm{SN}}(\mathbf{k})]$, and susceptibility for VBS order $[\chi_{\mathrm{VBS}}(\mathbf{k})]$ shown for $N = 10$ and $N = 14$, for the $\hat{H}_J$ model, Eq. (1) with $L = 48$. The Bragg peaks for SN (VBS) weaken (sharpen) with increasing $N$. The cartoon of the Brillouin zones shows the location of the ordering vectors of both order parameters. Quantitative finite size scaling of these orders is shown in Fig. 2.

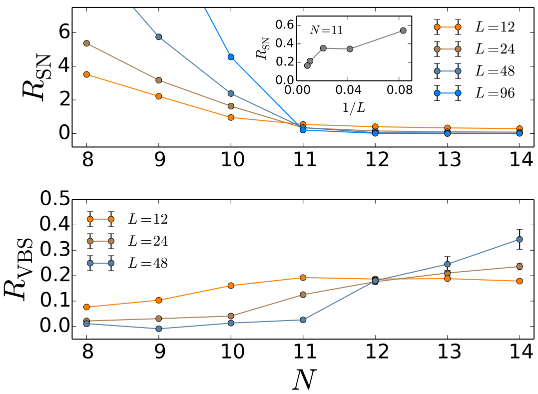


FIG. 2. Crossing plots of the ratios $R_{\mathrm{SN}}$ and $R_{\mathrm{VBS}}$ as a function of the discrete variable $N$ for the $\hat{H}_J$ model. It is seen that spin nematic order is present for $N \leq 10$. VBS order on the other hand is present for $N > 12$. $N = 12$ appears to be on the verge of VBS order. Interestingly, $N = 11$ has no SN or VBS order. In the text, we present evidence that this phase is a QSL. The inset in the upper panel shows $R_{\mathrm{SN}}$ scales to zero at $N = 11$, despite non-monotonic behavior at intermediate $L$.

Since $\hat{H}_J$ has SN order for $N = 3$ and is expected to have a non-magnetic VBS at large-$N$, it is interesting to ask what the nature of the transition at which SN magnetism is destroyed. The answer to this question is unclear based on current theoretical ideas and is best settled by unbiased numerical simulations. Exploiting that $\hat{H}_J$ has no sign problem we study it as a function of $N$ on $L \times L$ lattices at temperture $\beta$ by unbiased stochastic series expansion [29] quantum Monte Carlo simulations, with a previously described algorithm [24]. The SN state is described by the matrix order parameter $\hat{Q}_{\alpha\beta} = |\alpha\rangle\langle\beta| - \frac{1}{N}$. The static structure factor, $S_{\mathrm{SN}}(\mathbf{k}) = \frac{1}{N_{\mathrm{site}}}\sum_{ij} e^{i\mathbf{k}\cdot(\mathbf{r}_i - \mathbf{r}_j)}\langle \hat{Q}_{\alpha\alpha}(i)\hat{Q}_{\alpha\alpha}(j)\rangle$ is used to detect SN order. For the VBS order, we construct the $\mathbf{k}$ dependent susceptibility of dimer-dimer correlation functions in the usual way from imaginary time-displaced operators: $\chi_{\mathrm{VBS}}(\mathbf{k}) = \frac{1}{N_{\mathrm{site}}}\sum_{ij} e^{i\mathbf{k}\cdot(\mathbf{r}_i - \mathbf{r}_j)}\frac{1}{\beta}\int d\tau \langle \hat{P}_{\mathbf{r}_i,\mathbf{r}_i+\hat{x}}(\tau)\hat{P}_{\mathbf{r}_j,\mathbf{r}_j+\hat{x}}(0)\rangle$. Throughout this paper we have fixed $\beta = L$ for our finite size scaling [15].

As shown in Fig. 1, a peak in $S_{\mathrm{SN}}(\mathbf{k})$ is found at the Γ point. Comparing the data at $N = 10$ and $N = 14$, already qualitatively it is possible to see the peak in $S_{\mathrm{SN}}(\mathbf{k})$ softens as $N$ is increased. In contrast $\chi_{\mathrm{VBS}}(\mathbf{k})$ develops sharp peaks at the X and M points as $N$ is increased. These are precisely the momenta at which previous numerical studies of the triangular lattice quantum dimer model Eq. (3) have observed Bragg peaks [28], validating the large-$N$ mapping to Eq. (3) made earlier. To detect at which $N$, the magnetic order is destroyed and the VBS order first sets in, we study the ratio, $R_{\mathrm{SN}} = 1 - \frac{S_{\mathrm{SN}}(\mathbf{\Gamma}+\mathbf{a}2\pi/L)}{S_{\mathrm{SN}}(\mathbf{\Gamma})}$ (where $\mathbf{a} \equiv \mathbf{x} - \mathbf{y}/\sqrt{3}$) as a function of $L$. $R_{\mathrm{SN}}$ must diverge in a phase in which the Bragg peak height scales with volume and becomes infinitely sharp. On the other hand it must go to zero in a phase in which the correlation length is finite and the height and width of the Bragg peak saturate with system size. At a critical point standard finite size scaling arguments imply that the ratio, $R_{\mathrm{SN}}$ becomes volume independent. All of these facts together imply a crossing in this quantity for different $L$. Fig. 2 shows the $R_{\mathrm{SN}}$ and $R_{\mathrm{VBS}}$ ratios (an analogous quantity constructed for the VBS order from $\chi_{\mathrm{VBS}}(\mathbf{k})$ close to the **M**-point) as a function of the discrete variable $N$ for different $L$. The data for $R_{\mathrm{SN}}$ shows that the magnetic order is present for $N \leq 10$. The $R_{\mathrm{VBS}}$ data shows that the long-range VBS order is present for $N > 12$. From Fig. 2 we find that $N = 12$ is on the verge of developing VBS order; from the system sizes accesible we are unable to reliably conclude whether $N = 12$ has long range VBS order or not from our study. However, taken together the data show definitively that $N = 11$ has neither VBS nor SN order. As we shall substantiate below, at $N = 11$, $\hat{H}_J$ is a quantum spin-liquid (QSL).

*J-Q models:* In order to clarify the global phase diagram of SO($N$) anti-ferromagnets and access the quantum phase transitions between the SN, VBS and QSL phases found in $\hat{H}_J$, it is of interest to find an interaction that can tune between these phases at *fixed* $N$. In order to be meaningful, the new coupling must preserve all the symmetries of $\hat{H}_J$. To this end, we introduce and study a generalization of the four-site $Q$ term of SU(2) spins [30],

$$\hat{H}_Q = -Q \sum_{\langle ijkl\rangle} \left(\hat{P}_{ij}\hat{P}_{kl} + \hat{P}_{il}\hat{P}_{jk}\right) \quad (4)$$

where the sum includes elementary plaquettes of length four on the triangular lattice (with periodic boundary

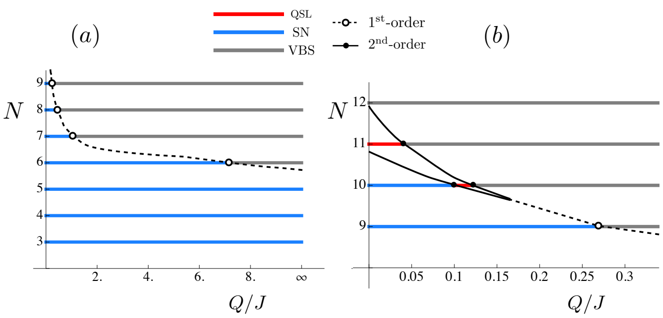


FIG. 3. Phase diagram of $\hat{H}_{JQ}$ [Eqs. (2,4)] for different values of $N$. The left panel shows the phase diagram for small $N$, where a first order SN-VBS transition is found for $6 \leq N \leq 9$, (see Fig. 4). As $N$ is increased we find the first order transition weakens. The right panel shows how an intermediate QSL phase emerges for $N = 10$ and $N = 11$. Transitions from the QSL to both SN and VBS phases are continuous on the large systems studied, see Fig. 5.

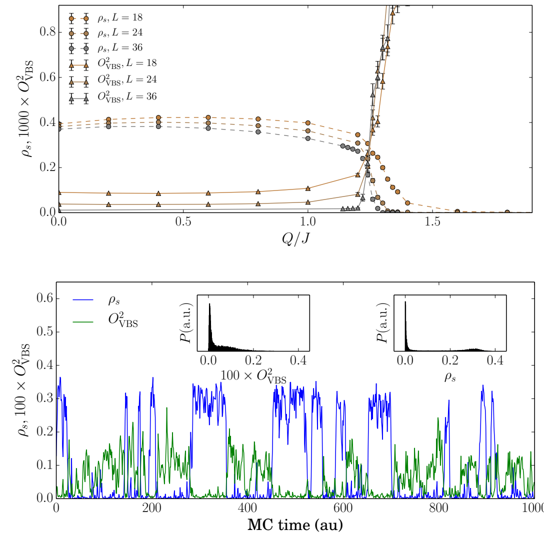


FIG. 4. First-order SN to VBS transition in $H_{JQ}$ at $N = 7$. The upper panel shows the VBS order parameter and the stiffness as a function for $Q/J$ for different $L$ indicating a direct SN-VBS transition. The lower panel shows MC histories (and histograms in the inset) at $Q/J = 1.26$, providing clear evidence that the SN-VBS transition at $N = 7$ is direct and first-order.

conditions on an $L \times L$ system there are $3L^2$ such plaquettes). For a fixed-$N$, $\hat{H}_Q$ provides a tuning parameter which preserve both the internal and lattice symmetries of $\hat{H}_J$ and hence allows us to study the generic phase diagram of SO($N$) magnets. A summary of the phase diagram of $\hat{H}_{JQ}$ in the $N$-$Q/J$ plane is in Fig. 3: The $Q$-interaction destroys the SN order and gives way to VBS order only for $N \geq 6$. We have found evidence for direct first-order SN-VBS transitions for $6 \leq N < 10$ and exotic continuous SN-VBS transitions for $N = 10$ and $N = 11$.

As an example of our observed first-order behavior we present in Fig. 4, our study of the $N = 7$ QMC data for the spin stiffness $\rho_s \equiv \langle W_x^2 \rangle / L$ (where $W_x$ is the winding number of the spin world lines), which acts as a sensitive order parameter for the SN phase, and the VBS order parameter $O^2_{\rm VBS} \equiv \chi_{\rm VBS}(\mathbf{M})/N_{\rm site}$. Clear evidence for a direct first order SN-VBS transition at $N = 7$ is found.

The nature of the transition changes at $N = 10$, where evidence for two phase transitions is found. As shown in Fig. 5 the SN order vanishes at a $Q/J$ smaller than the value at which VBS order develops. Although the difference is small for $N = 10$, it is significant. The data for $N = 11$ in Fig. 5 shows that the SN and VBS orders do not vanish at the same point. In fact $R_{\rm SN}$ indicates that the SN order has vanished already at $Q/J = 0$, consistent with our previous analysis of $\hat{H}_J$. As illustrated by the dashed and solid lines in Fig. 3, the appearance of the QSL phase is consistent with a global phase diagram for the SO($N$) magnets.

*QSL phase and criticality:* We have identified the ground state between SN and VBS as a QSL, since it does not show evidence for any Landau-order. Were the intermediate phase characterized by a conventional order parameter, we would have expected strong first order transitions of the kind between SN and VBS (see Fig. 4), instead we find continuous transitions.

There are field theoretic reasons to expect a QSL on quantum disordering a spin nematic. The long-distance description of our SO($N$) models is given by a RP$^{N-1}$ theory (in contrast to the CP$^{N-1}$ description of SU($N$) models [31]), which can be described as $N$ real matter fields coupled to a $Z_2$ gauge field. Such a theory is expected to host three phases [32], a symmetry breaking phase in which the matter condenses (which we identify in our spin model as the SN), a stable phase in which the matter gets a gap and the $Z_2$ gauge theory is deconfined (identified here as the QSL) and a phase in which matter is gapped and the $Z_2$ is confined (identified here as the VBS). Thus, the SN-QSL critical point should be in the universality class of O($N$)$^*$ critical point [3]. The QSL-VBS phase transition should be in the same universality class as the critical point between these identical phases in the quantum dimer model since the magnetic fluctuations are gapped in both the QSL and VBS phases. A previous analysis of this phase transition has predicted an O(4)$^*$ phase transition [27], where the VBS order parameter is identified with a bilinear of the primary field.

A detailed study of the critical phenomena at $N = 10$ and $N = 11$ is clearly beyond the scope of the current manuscript. We shall be satisfied here with a brief analysis: At the QSL-VBS critical point, we are able to carry out reasonable data collapses [15] at both $N = 10$ and

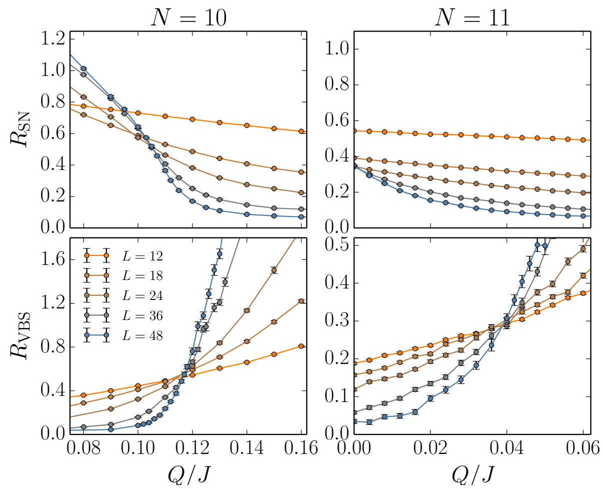


FIG. 5. Crossings of $R_{\rm SN}$ (above) and $R_{\rm VBS}$ (below) signaling the location of the onset of long-range SN and VBS orders at $N = 10$ (left) and $N = 11$ (right). At $N = 10$, $R_{\rm SN}$ and $R_{\rm VBS}$ cross at close but significantly different couplings, $Q_c = 0.100(5)$ and $Q_c = 0.117(2)$ respectively. At $N = 11$, $R_{\rm SN}$ appears to have crossed at $Q/J < 0$ (we cannot study this region because of the sign problem), whereas $R_{\rm VBS}$ crosses at $Q_c = 0.042(3)$. From the location of the crossings, for both $N = 10$ and $N = 11$, we can infer an intermediate phase which is neither SN nor VBS, as shown in Fig. 3(b). We present arguments that this phase is a QSL. No direct evidence for first order behavior is found at either of the transitions, though a weakly first order SN-QSL cannot be ruled out. The QSL-VBS transitions shows good scaling behavior with unconventional critical exponents.

$N = 11$ for $O^2_{\rm VBS}$ (for both X and M ordering vectors, see Fig. 1) and $R_{\rm VBS}$, where we find, $\eta_{\rm VBS} = 1.3(2)$ and $\nu_{\rm VBS} = 0.65(20)$ for the anomalous dimension of $O_{\rm VBS}$. The unusually large value of $\eta_{\rm VBS}$ is a direct consequence of fractionalization in the intermediate QSL phase and is often regarded as a smoking gun diagnostic of exotic critical points (see e.g., [33]). More quantitatively, our critical exponents are in rough agreement with the best estimate of $\eta = 1.375(5)$ of the bilinear field and $\nu = 0.7525(10)$ in the O(4) model [34]. We note that the values for $\eta_{\rm VBS}$ and $\nu_{\rm VBS}$ agree within the quoted errors for $N = 10$ and $N = 11$. Taken together, this bolsters the case that the intermediate QSL phase has $Z_2$ fractionalization, albeit more work is needed for a definitive identification. Unfortunately, the SN-QSL transition, observed only at $N = 10$, has large corrections to scaling and we are unable to reliably determine its critical exponents or determine whether it is a weakly first order transition (no direct evidence for a first-order transition has been found of the type shown for the $N = 7$ case).

In summary, we have introduced a new family of sign-free SO($N$) spin models, which can be regarded as non-bipartite generalizations of their popular SU($N$) cousins. The triangular lattice model which we have studied thoroughly here hosts a spin nematic, a VBS with a large unit cell, a quantum spin liquid phase and unusual quantum critical points. The absence in the SO($N$) models of a direct continuous "deconfined quantum critical point" [33] is in striking contrast to previous simulations of the related bipartite SU($N$) models [8, 23]. We have offered a plausible field theoretic scenario that naturally explains this difference. It is interesting that the absence (presence) of a QSL in bipartite SU($N$) (non-bipartite SO($N$)) spin models seems to track the absence or presence of this phase in the kind of quantum dimer models that our model maps to at large-$N$ [35].

While the study in this paper has focussed on the triangular lattice, our family of models, Eq. (2,4) may be constructed sign free on any two or three dimensional non-bipartite lattice. Because of the larger degree of frustration, the kagome system may provide a wider swath of the QSL phase and hence could possibly allow a more detailed study of this phase, even if the phase diagram is of the same form found here. Exploring the phase diagram and quantum phase transitions of the three dimensional pyrochlore system is an exciting open direction for future work.

The author is grateful to J. Chalker, T. Lang, M. Levin, R. Mong, G. Murthy, A. Nahum, A. Sandvik, T. Senthil and M. Zaletel for helpful discussions. This research was supported in part by NSF DMR-1056536.

[1] L. Balents, Nature **464**, 199 (2010), URL http://dx.doi.org/10.1038/nature08917.
[2] S. Sachdev, *Quantum Phase Transitions* (Cambridge University Press, 1999).
[3] C. Xu, Int. J. Mod. Phys. B p. 1230007 (2012).
[4] C. Wu, Physics **3**, 92 (2010).
[5] B. Sutherland, Phys. Rev. B **12**, 3795 (1975), URL http://link.aps.org/doi/10.1103/PhysRevB.12.3795.
[6] I. Affleck, Phys. Rev. Lett. **54**, 966 (1985), URL http://link.aps.org/doi/10.1103/PhysRevLett.54.966.
[7] N. Read and S. Sachdev, Phys. Rev. Lett. **62**, 1694 (1989), URL http://link.aps.org/doi/10.1103/PhysRevLett.62.1694.
[8] R. K. Kaul, R. G. Melko, and A. W. Sandvik, Annu. Rev. Cond. Matt. Phys **4**, 179 (2013), URL http://www.annualreviews.org/doi/abs/10.1146/annurev-conmatphys-030212-184215.
[9] N. Read and S. Sachdev, Phys. Rev. Lett. **66**, 1773 (1991), URL http://link.aps.org/doi/10.1103/PhysRevLett.66.1773.
[10] E. Demler, W. Hanke, and S.-C. Zhang, Rev. Mod. Phys. **76**, 909 (2004), URL http://link.aps.org/doi/10.1103/RevModPhys.76.909.
[11] H.-H. Tu, G.-M. Zhang, and T. Xiang, Phys. Rev. B **78**, 094404 (2008), URL http://link.aps.org/doi/10.1103/PhysRevB.78.094404.
[12] F. Alet, S. Capponi, H. Nonne, P. Lecheminant, and I. P. McCulloch, Phys. Rev. B **83**, 060407 (2011), URL http://link.aps.org/doi/10.1103/PhysRevB.83.060407.

[13] K. Okunishi and K. Harada, Phys. Rev. B **89**, 134422 (2014), URL http://link.aps.org/doi/10.1103/PhysRevB.89.134422.

[14] Strictly speaking the symmetry of our model is an SO($N$) for odd-$N$ and an O($N$)/$Z_2$ for even $N$. This point is discussed further in the supplementary materials.

[15] Please refer to supplementary materials for more details on the model and the numerical simulations.

[16] G. Santoro, S. Sorella, L. Guidoni, A. Parola, and E. Tosatti, Phys. Rev. Lett. **83**, 3065 (1999), URL http://link.aps.org/doi/10.1103/PhysRevLett.83.3065.

[17] K. Harada, N. Kawashima, and M. Troyer, Phys. Rev. Lett. **90**, 117203 (2003), URL http://journals.aps.org/prl/abstract/10.1103/PhysRevLett.90.117203.

[18] K. S. D. Beach, F. Alet, M. Mambrini, and S. Capponi, Phys. Rev. B **80**, 184401 (2009), URL http://link.aps.org/doi/10.1103/PhysRevB.80.184401.

[19] J. Lou, A. Sandvik, and N. Kawashima, Phys. Rev. B **80**, 180414 (2009), URL http://link.aps.org/doi/10.1103/PhysRevB.80.180414.

[20] R. K. Kaul, Phys. Rev. B **85**, 180411 (2012), URL http://link.aps.org/doi/10.1103/PhysRevB.85.180411.

[21] R. K. Kaul and A. W. Sandvik, Phys. Rev. Lett. **108**, 137201 (2012), URL http://link.aps.org/doi/10.1103/PhysRevLett.108.137201.

[22] M. S. Block and R. K. Kaul, Phys. Rev. B **86**, 134408 (2012), URL http://link.aps.org/doi/10.1103/PhysRevB.86.134408.

[23] M. S. Block, R. G. Melko, and R. K. Kaul, Phys. Rev. Lett. **111**, 137202 (2013), URL http://link.aps.org/doi/10.1103/PhysRevLett.111.137202.

[24] R. K. Kaul, Phys. Rev. B **86**, 104411 (2012), URL http://link.aps.org/doi/10.1103/PhysRevB.86.104411.

[25] A. Laeuchli, F. Mila, and K. Penc, Phys. Rev. Lett. **97** (2006).

[26] N. Read and S. Sachdev, Nuclear Physics B **316**, 609 (1989), ISSN 0550-3213, URL http://www.sciencedirect.com/science/article/pii/0550321389900618.

[27] R. Moessner and S. L. Sondhi, Phys. Rev. B **63**, 224401 (2001), URL http://link.aps.org/doi/10.1103/PhysRevB.63.224401.

[28] A. Ralko, M. Ferrero, F. Becca, D. Ivanov, and F. Mila, Phys. Rev. B **74**, 134301 (2006), URL http://link.aps.org/doi/10.1103/PhysRevB.74.134301.

[29] A. W. Sandvik, AIP Conf. Proc. **1297**, 135 (2010), URL http://scitation.aip.org/content/aip/proceeding/aipcp/10.1063/1.3518900.

[30] A. W. Sandvik, Phys. Rev. Lett. **98**, 227202 (2007), URL http://link.aps.org/doi/10.1103/PhysRevLett.98.227202.

[31] N. Read and S. Sachdev, Phys. Rev. B **42**, 4568 (1990).

[32] P. E. Lammert, D. S. Rokhsar, and J. Toner, Phys. Rev. Lett. **70**, 1650 (1993), URL http://link.aps.org/doi/10.1103/PhysRevLett.70.1650.

[33] T. Senthil, A. Vishwanath, L. Balents, S. Sachdev, and M. P. A. Fisher, Science **303**, 1490 (2004), URL http://www.sciencemag.org/content/303/5663/1490.abstract.

[34] H. Ballesteros, L. Fernndez, V. Martn-Mayor, and A. M. Sudupe, Physics Letters B **387**, 125 (1996), ISSN 0370-2693, URL http://www.sciencedirect.com/science/article/pii/0370269396009847.

[35] R. Moessner and S. L. Sondhi, Phys. Rev. Lett. **86**, 1881 (2001), URL http://link.aps.org/doi/10.1103/PhysRevLett.86.1881.